

Submitted to JO SA A.

PROPERTIES OF PHOTONIC CRYSTAL FIBER AND THE EFFECTIVE INDEX MODEL

J. C. KNIGHT, T. A. BIRKS, P. ST. J. RUSSELL

OPTOELECTRONICS GROUP, SCHOOL OF PHYSICS, UNIVERSITY OF BATH

BATH BA2 7AY

UNITED KINGDOM

FAX Int+44-1225-826-110

email: j.c.knight@bath.ac.uk

J.-P. DE SANDRO

OPTOELECTRONICS RESEARCH CENTRE, UNIVERSITY OF SOUTHAMPTON

SOUTHAMPTON, SO17 1BJ

UNITED KINGDOM

ABSTRACT

We report on the waveguiding properties of a new type of low-loss optical waveguide. The photonic crystal fiber can be engineered to support only the fundamental guided mode at every wavelength within the transparency window of silica. Experimentally, a robust single mode has been observed over a wavelength range from 337nm to beyond 1550nm (restricted only by available wavelength sources). By studying the number of guided modes for fibers with different parameters and the use of an effective index model we are able to quantify the requirements for monomode operation. The requirements are independent of the scale of the fiber for sufficiently short wavelengths. Further support for the predictions of the effective index model is given by the variation of the spot size with wavelength.

INTRODUCTION

By periodically structuring a material in two or three dimensions with a pitch of the order of the optical wavelength one can fabricate new optical materials with unusual properties. Such *photonic crystal* materials are a topic of active research world-wide because of their potential importance in the development of novel optoelectronic devices.¹ The relevance of these materials arises from the possibility of controlling light in new and useful ways. They present an opportunity to engineer specific desired properties into the material at the design stage. One of the most cited application areas is in the design of novel waveguides with unusual properties, and several research groups have studied this possibility theoretically.²⁻⁴ We recently demonstrated the first low-loss monomode waveguide based on the use of a two-dimensional photonic crystal material.⁵ This is in the form of a fine silica fiber which has a hexagonal array of air holes running down its length. This photonic crystal fiber (PCF) can easily be made many meters in length. The pitch of the hexagonal crystal pattern is in the range of 1-10 μ m. By leaving a single lattice site without an air hole, one can form a localized region which effectively has a higher refractive index than the rest of the structure (figure 1). This acts as a waveguide core in which it is possible to trap light traveling almost parallel to the fiber axis. Thus, in contrast to the photonic crystal waveguide designs which have previously been investigated theoretically, our waveguide does not rely on photonic band gap effects. Partly as a result of this the guided mode is easily observed. However, given that this design uses the photonic crystal as an "effective index material" to form a waveguide cladding one might imagine that it would share many of the properties of conventional optical fibers. We have previously reported⁵ the extraordinarily broad spectral range of monomode operation of this fiber. We have also reported how an effective index model arising from this observation can explain the surprising phenomenon of a short-wavelength bend loss edge in this fiber and prove that the fiber can indeed be monomode at all wavelengths.⁶ In this paper we quantify how the number of guided modes in the structure depends on the design parameters. We show that some

of the properties of this type of waveguide differ radically from those familiar from optical fiber waveguide theory. Indeed, the photonic crystal fiber represents a new class of optical waveguide which allows greater freedom in the waveguide design than can be achieved using conventional materials.

EFFECTIVE V-VALUE AND NUMBER OF GUIDED MODES

Our waveguide is formed by a hexagonal array of air holes embedded in a silica matrix, and is represented schematically in figure 1. We refer to the centre-to-centre spacing between the nearest air holes as the pitch Λ and the air hole diameter as d . Our fiber has a hexagonal cross-section and typically about 300 air holes. Such a fiber can be fabricated using a stack-and-draw procedure, as has been described previously.^{5,7} A single missing air hole forms a defect site in the periodic material, and constitutes the waveguide core. (A core could as easily be formed by leaving out more than one air hole, or by using instead a smaller air hole at a single or several lattice sites. These structures can probably also be made to be monomode, but we do not consider such geometries here.) The choice of a definition of the size of the waveguide core is not intuitively obvious, and is to a certain extent arbitrary. We shall use the pitch Λ as the core radius.

We have observed experimentally that certain lengths of PCF support only a single guided mode over the spectral range from at least $\lambda=337\text{nm}$ to well beyond $\lambda>1550\text{nm}$. (The measurement is limited by the sources available to us.) We know this from observations of the near- and far-field patterns of the guided mode at different wavelengths, which are very similar and are independent of the way light is coupled into the structure and of any bends or twists in the fiber. This represents monomode waveguiding over most of the transmission window of silica, and is a startling feature which appears to be unique to this structure. In a conventional fiber waveguide a combination of refractive index and core size which guides a single robust mode at 1550nm would be expected to guide several modes at 337nm.⁸ This does not occur in

PCF only because of the unusual interaction of the guided mode with the photonic crystal cladding material. The observed effect can be understood qualitatively by considering the imaging capabilities of light of a wavelength λ . In the long wavelength limit, where λ is far greater than the characteristic distance scales of the photonic crystal (d and Λ), the optical field in the cladding region can only be very weakly modulated by the air holes, and the cladding can be thought of as a homogeneous material with an average index n_{avg} defined as the area-average of the squares of the refractive indices.⁹ In this case the fiber is expected to act much as a conventional optical fiber. However, for shorter wavelengths (when $\lambda \approx d$) the field distribution in the cladding moves increasingly out of the air holes (the guided mode will, of course, be evanescent in air) and these begin to form sharp minima in the field pattern. This effect is illustrated in figure 2 where we present contour plots of the observed near-field patterns of the guided mode at the long wavelength end of our measurements ($\lambda=1.55\mu\text{m}$) and at a rather shorter wavelength ($\lambda=0.458\mu\text{m}$). These plots (which were recorded by a vidicon camera) show the modal intensity distribution in the cladding region of the fiber being sharply modulated by the presence of the air holes at 458nm, but far less so at 1.55 μm . This concentration of the field in the high-index silica regions at shorter wavelengths has the effect of increasing the effective refractive index $n_{eff} > n_{avg}$ of the cladding medium and reducing the index difference between the core and the cladding. At the same time, the wavelength of the light becomes significantly smaller than the spacing between the air holes, and one might imagine that the guided mode would start to leak away from the core along the silica bridges between the holes. On the other hand, it is experimentally observed that the fundamental mode remains guided down to at least $\lambda < \Lambda/15$, while higher-order guided modes do not appear. In a conventional optical fiber⁷ the value of the normalized frequency V given by

$$V = \frac{2\pi\rho}{\lambda} (n_{co}^2 - n_{cl}^2)^{1/2} \quad (1)$$

determines the number of waveguide modes. A low value of V ($V < 2.405$) implies monomode waveguiding: as V increases so more and more modes are guided in the waveguide core. The fact that in PCF n_{cl} in eqn. (1) is strongly dependent on λ implies very different behavior of V in this case.

We can gain more quantitative insight into this effect by generalizing the ideas of conventional waveguides to account for the microstructured cladding region. We assume in the effective refractive index model⁶ that the waveguide consists of a core and a cladding material which have refractive indices n_{co} and n_{cl} . The core in our waveguide is pure silica, and $n_{co} = n_{silica}$. However the definition of the refractive index of the cladding material is not as straightforward. Remembering that $n_{co}k > \beta > n_{cl}k$ for the propagation constant β of a guided mode (where k is the free-space propagation constant of light of wavelength λ), we recognize that the index of the cladding region can be defined in terms of the propagation constant of the lowest mode which could propagate in the infinite cladding material. This lowest mode has the largest allowed value of β , zero transverse wavevector, and fills all of space. We refer to it as the fundamental space-filling mode. We can then define the effective index of the cladding material as $n_{eff} = \beta_{FSM} / k$. This definition of the cladding index is general in that it is independent of the presence of the core. Clearly its utility is restricted to when the material is being used in the “total external reflection” regime as a waveguide cladding. It remains to calculate the value of β_{FSM} for the structure being considered here. This is readily done, as we know the approximate form of the field distribution for this mode. Some details of the calculation are given in reference 6.

Having computed n_{eff} we can calculate an effective V -value for PCF. The resulting curves showing the variation of the effective V -value V_{eff} (defined as in equation 1 with $n_{cl} = n_{eff}$) with λ/Λ are plotted in figure 3 for 5 different values of d/Λ . V_{eff} increases from zero at relatively

long wavelengths, before leveling out and approaching a fixed value for much shorter wavelengths and larger structures. This is in sharp contrast to the case of a conventional optical fiber, for which V rises without limit as one decreases the wavelength or increases the core size, resulting inevitably in the guidance of higher-order modes (see equation 1). Figure 3 implies that it is possible to design a fiber which will be monomode for any wavelength, no matter how short. The exact design parameters needed for such a fiber are not predicted by the effective index model: the absolute values of V_{eff} in figure 3 are rather arbitrary, not least because they depend on an arbitrary choice of a value for the core radius. Nonetheless, we expect that there should be a value of V_{eff} (a horizontal line on figure 3) which will represent the cut-off value V_{co} for the guidance of higher-order modes. Curves on figure 3 which never pass above this line would represent fibers which were always monomode. On the other hand, curves which remain far below this line would represent poorly guiding fibers, and would suffer from excessive bend loss. The ideal monomode PCF would have a value of d/Λ such that the V_{eff} curve rose to just below V_{co} .

A natural question to ask is what is the numerical value of V_{co} ? In order to determine this experimentally we have made a study of the near and far field patterns of several fibers with different values of pitch and air filling fraction, at a number of different wavelengths. We find that for fibers with sufficiently large values of d/Λ we can indeed observe more than a single guided mode. Figure 4 shows a contour map of the near-field pattern of a second-order mode in such a fiber, selectively excited by adjusting the input conditions. As with the fundamental mode, the modal intensity pattern shown in figure 4 is very similar to the corresponding pattern in a conventional circularly-symmetric fiber, but modulated by the hexagonal array of air holes. The positions of some of the nearest air holes to the core are evident in the intensity distribution. Based on figure 3, fibers with a constant d/Λ are expected to support only a single mode over a large range of values of Λ/λ , if $V_{eff} < V_{co}$. By classifying fibers according to

whether or not they are monomode we are able to determine the approximate value of V_{co} . The measured points are plotted on figure 3. We have used scanning electron micrographs of the cleaved fiber sections to determine the values of Λ/λ and d/Λ for each fiber investigated. In this way we are able to read off a value for V_{eff} for each fiber from the theoretical curves such as those in figure 3. The results are also summarized in table 1. The data support the idea that there should be a single value for V_{co} , and show that this cut-off is around $V_{eff} \approx 2.5$. This value is very close to the familiar $V_{co} = 2.405$ found in conventional fibers. This is reassuring but should be considered to be at least partly coincidental, given the arbitrary choice of definition of the core size in our case. Within the effective index model a fiber with $V_{eff} < 2.5$ can be expected to support but a single mode, which enables us to estimate the range of monomode operation for a particular fiber. Some fibers have $V_{eff} < 2.5$ always, and these will always be monomode. The critical value of the parameter d/Λ below which this occurs is $d/\Lambda = 0.2$. It should be stressed that this prediction is only valid within the assumptions of the effective index model: nonetheless the experimental results shown in figure 3 allow one to predict with some confidence that a fiber with $V_{eff} < 2.5$ will support only a single mode.

Figure 3 also illustrates experimentally how Λ/λ , and hence the overall scale of the structure including the core size, can be varied by over an order of magnitude while maintaining monomode waveguiding in an otherwise identical structure (we predicted this behavior in reference 5). This means the PCF structure can be used to design an ultra-large mode area fiber. In theory a monomode photonic crystal fiber could be scaled up many orders of magnitude in dimension, with no other change in the fiber design, and maintain monomode waveguiding. As we have described,⁶ the useful range of the fiber is eventually limited by bend loss, which occurs in this case on both the long and the short wavelength edges of the transmission band.

FAR FIELD PATTERN AND SPOT SIZE

Far-field measurements of the normalized half-intensity angle have been used to infer the V -value for conventional monomode optical fibers. It has been shown¹⁰ that in the case of a conventional step-index fiber with a core radius ρ there is a monotonic relationship between the value of $k\rho \sin(\theta_h)$ and the normalized frequency V . Here, θ_h represents the half-maximum angle of the far-field intensity distribution of the fundamental guided mode. This relationship is represented by the solid curve in figure 5 (plotted using the upper axis). In conventional fibers, only a small range of V -values is available to verify this relationship: such measurements as have been made are in good agreement with the theoretical predictions.¹⁰ Assuming that measurements are done on a single fiber with a fixed value of core radius ρ , and neglecting the small effects due to the chromatic dispersion of silica, varying the normalized frequency is equivalent to varying the wavelength. To investigate the variation of the far-field pattern with wavelength in the photonic crystal fiber we have measured the half-intensity angle at a number of wavelengths over the transmission band of the fiber. This is readily done using different laser sources, and over a much broader range than is possible with a conventional optical fiber due to the intrinsically monomode nature of the waveguiding in the present case. Measurements were taken of the 10% and 50% points in the intensity pattern, along both of the high-symmetry directions in the field pattern. We obtained very similar results for the two orientations, and results from only one of these will be presented. The fiber used to make these measurements had $\Lambda=2.3\mu\text{m}$, $d=0.5\mu\text{m}$.

The results are plotted as points on figure 5, using the bottom axis. The relative scales of the upper and lower axes are chosen so that they correspond in the long wavelength limit, when $n_{cl}=n_{avg}$ (see eqn. 1). It should be remembered that we have made a somewhat arbitrary (though consistent) choice of value for the core radius. Nonetheless, it is clear that at the longer wavelength end of our measurements (i.e., for small V) the values and the trend of the observed

points are similar to those predicted for a conventional optical fiber with the average index difference. Considering that the guided mode is not circularly symmetric the agreement is very good. This supports the prediction of the effective index model that for a fiber with the above parameters the effective index at $\lambda=1.55\mu\text{m}$ is quite close to the long wavelength limit. ($V_{\text{eff}}=1.58$ compared to $V_{\text{avg}}= 2.09$, where V_{avg} is defined as in equation (1) but with $n_{\text{cl}}=n_{\text{avg}}$). On the other hand, for smaller values of the wavelength the differences between the plotted points and the solid curve become more pronounced, the experimental points flattening out at a value around unity (with some fluctuations). The effective index model predicts that the V -value will reach a limiting value for small wavelengths - the broken line on figure 5 again shows the variation of the predicted $k\rho \sin(\theta_h)$, but now plotted using the lower axis and accounting for the variation of V_{eff} with wavelength. This curve shows that for PCF the values of $k\rho \sin(\theta_h)$ are expected to level off around unity. Although the measured points do not fall directly on the curve, the agreement is nonetheless quite good. There is a systematic offset between the observations and the theoretical curve, possibly due to our choice of definition of θ_h or of the core size. The fluctuation present on the experimental data for shorter wavelengths appears to be a real effect which is not predicted by the effective index model. It might be associated with variations in the sizes and shapes of the air holes in the immediate vicinity of the fiber core.

CONCLUSIONS

We have described a low-loss optical fiber based on the use of a two-dimensional silica-air photonic crystal material as the fiber cladding. The fiber core is formed by a single lattice site in the crystal which is pure silica (no air). The theoretical and experimental results presented here show that the number of guided modes in PCF is determined by the geometry of the structure, being quite independent of the scale of the structure for sufficiently large structures or short wavelengths. The critical parameter is shown to be the ratio of the air hole diameter d

to the spacing between adjacent holes Λ . By experimentally determining the value of d/Λ which allows a second guided mode we are able to design a photonic crystal fiber which will be monomode for any wavelength or scale of structure. Similarly, it is possible to design a fiber which would support only 2 guided modes for any wavelength shorter than a critical value. We have confirmed these predictions, as far as possible, with real structures.

The photonic crystal fiber is an interesting form of optical waveguide with some novel and potentially useful properties. For example, the super-broad range of monomode operation might have applications in frequency doubling or tripling experiments in optical fibers. The dispersion properties of the fiber are expected to exhibit some unusual features. The fiber could be used as a large mode area fiber for fiber amplifiers or high intensity light transmission. Interesting experiments remain to be done using the PCF to study the interaction between light trapped in a guided mode and a liquid or gas in the air holes. Moreover, we believe that similar effects could be used to advantage in different material systems and with different objectives.

This work is supported by the Engineering and Physical Sciences Research Council, U.K. Additional support from DERA Malvern, U.K. is gratefully acknowledged. T. A. Birks is a Royal Society University Research Fellow.

References

1. See e.g. the special issues of Journ. Opt. Soc. Am. B **10**, 279-413, edited by C. M. Bowden, J. P. Dowling and H. O. Everitt (1993), J. Mod. Opt. **41**, 2 edited by G. Kurizki and J. W. Haus (1994) and *Microcavities and Photonic Bandgaps: Physics and Applications*, J. G. Rarity and C. Weisbuch, eds. (Kluwer, Dordrecht, 1996)
2. A. Mekis, J. C. Chen, I. Kurland, S. H. Fan, P. R. Villeneuve, J. D. Joannopoulos, "High transmission through sharp bends in photonic crystal waveguides," Phys. Rev. Lett. **77**, 3787-3790 (1996); J. D. Joannopoulos, R. D. Meade, J. N. Winn, *Photonic crystals: molding the flow of light*, (Princeton University Press, Princeton, N.J. 1995)
3. D. M. Atkin, P. St. J. Russell, T. A. Birks and P. J. Roberts, "Photonic band structure of guided Bloch modes in high index films fully etched through with periodic microstructure," J. Mod. Opt. **43**, 1035-1053 (1996), P. St. J. Russell, D. M. Atkin, T. A. Birks and P. J. Roberts, "Bound modes of two-dimensional photonic crystal waveguides" in *Microcavities and Photonic Bandgaps: Physics and Applications*, J. G. Rarity and C. Weisbuch, eds., (Kluwer, Dordrecht, 1996)
4. T. A. Birks, P. J. Roberts, P. St. J. Russell, D. M. Atkin, and T. J. Shepherd, "Full 2-d photonic bandgaps in silica/air structures," Elect. Lett. **31**, 1941-1943 (1995)
5. J. C. Knight, T. A. Birks, P. St. J. Russell and D. M. Atkin, "All-silica single-mode optical fiber with photonic crystal cladding," Opt. Lett. **21**, 1547-1549 (1996); see also errata Opt. Lett. **22**, 484-485 (1997)
6. T. A. Birks, J. C. Knight and P. St. J. Russell, "Endlessly single-mode photonic crystal fiber," Opt. Lett. **22**, 961-963 (1997)
7. R. J. Tonucci, B. L. Justus, A. J. Campillo and C. E. Ford, "Nanochannel array glass," Science **258**, 783-785 (1992), A. Rosenberg, R. J. Tonucci, H. B. Lin, and A. J. Campillo, "Near-infrared 2-dimensional photonic band-gap materials," Opt. Lett. **21**, 830-832 (1996)

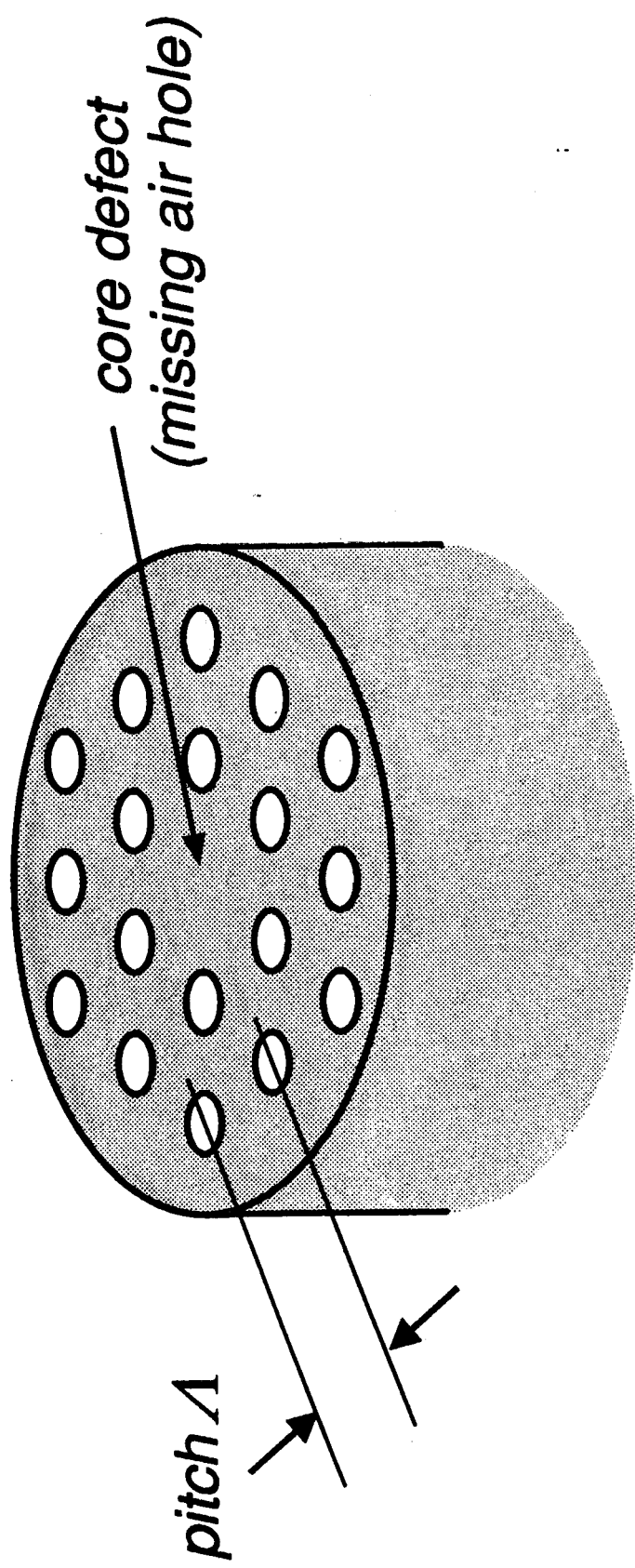
8. A. W. Snyder and J. D. Love, *Optical Waveguide Theory* (Chapman & Hall, New York, 1983)
9. D. E. Aspnes "Local-field effects and effective-medium theory: A microscopic perspective," *Am. J. Phys.* **50**, 704-709 (1982)
10. W. A. Gambling, D. N. Payne, H. Matsumura and R. B. Dyott, "Determination of core diameter and refractive-index difference of single-mode fibres by observation of the far-field pattern," *Microwaves, Optics and Acoustics* **1**, 13-17 (1976)

d (μm)	Λ (μm)	λ (μm)	d/Λ	Λ/λ	V_{eff}	No. of modes
1.1	10.0	.633	0.11	16.	1.95	1
0.5	2.3	1.55	0.22	1.5	0.99	1
0.5	2.3	0.633	0.22	3.6	2.25	1
0.4	2.8	0.633	0.15	4.4	1.96	1
1.4	4.9	1.55	0.29	3.1	2.59	2
1.4	4.9	0.633	0.29	7.7	2.93	2
1.9	9.5	0.633	0.20	15.	2.53	2

TABLE 1 Parameters of some photonic crystal fibers observed to support one or two modes.

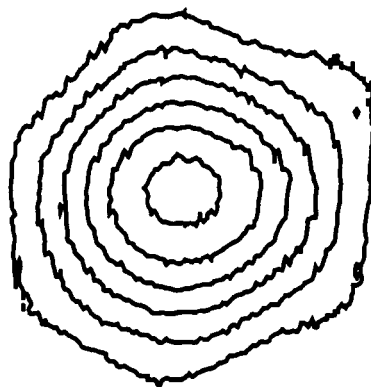
FIGURE CAPTIONS

- Figure 1. Schematic diagram of the silica/air photonic crystal fiber being discussed. A typical fiber has around 300 air holes arranged in a hexagonal pattern, and is many meters long.
- Figure 2. Near field contour maps of the fundamental guided mode in a PCF at the two different wavelengths $\lambda=458\text{nm}$ and $\lambda=1.55\mu\text{m}$. The spacing between the air holes (and hence the core radius) in the fiber used here is approximately $\Lambda=2.3\mu\text{m}$, and $d/\Lambda=0.23$.
- Figure 3. The effective normalized frequency V_{eff} plotted versus Λ/λ (curves) for several different values of d/Λ , and experimental points for the several different fibers described in table 1. Circles represent observed monomode fibers, while the squares show fibers supporting more than a single mode.
- Figure 4. Near-field map of a second-order mode selectively excited in a fiber with $\Lambda=4.9\mu\text{m}$ and $d/\Lambda=0.29$.
- Figure 5. Dependence of spot size on wavelength for a conventional optical fiber (solid curve) and a PCF (points). The axes are scaled so that they correspond in the long wavelength limit where $n_{cl}=n_{avg}$. The dotted curve shows the conventional result corrected for the variation of V_{eff} with wavelength.





$\lambda=458\text{nm}$



$\lambda=1550\text{nm}$

